ASEAN Engineering Journal

Full Paper

ESTIMATING AND ANALYZING COVID-19 TRANSMISSION IN THAILAND THROUGH DEEP NEURAL NETWORK

Rati Wongsathan[a]*, Wutthichai Puangmanee[b]

[a]Department of Electrical Engineering, Faculty of Engineering and Technology, 50230, Chiang Mai, Thailand
[b]Department of Computer Engineering, Faculty of Engineering and Technology, 50230, Chiang Mai, Thailand

Article history
Received
24 March 2023
Received in revised form
25 July 2023
Accepted
08 August 2023
Published online
29 February 2024

*Corresponding author
rati@northcm.ac.th
r

Graphical abstract

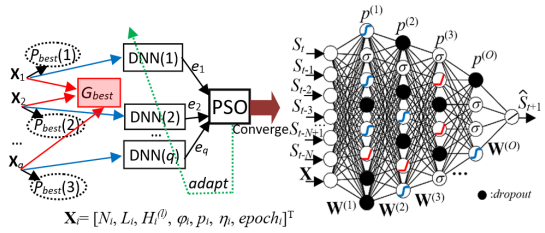

Abstract

The COVID-19 pandemic has caused significant global suffering and mortality, and effective control measures have been elusive. This study aims to develop an accurate and reliable prediction model using deep neural networks (DNN) to estimate the epidemic size and trends of COVID-19 cases, as well as the effective reproduction number, *R*(*t*). The efficacy of various control measures for COVID-19 has been questioned, and an efficient prediction model can aid in decision-making and planning. Overfitting is a common issue in neural networks, which can limit their accuracy and reliability. A modified dropout regularization technique and particle swarm optimization (PSO) are employed to enhance the accuracy of the DNN. The proposed model outperforms conventional neural networks and previous studies in terms of accuracy and reliability. The estimated *R*(*t*) values are consistent with measured values, which demonstrates the usefulness of this model in analyzing the situation and informing effective intervention strategies. The developed dropout-DNN-PSO model is an accurate and reliable predictor of COVID-19 trends and *R*(*t*) values. It can aid decision-makers in planning and implementing effective control measures. The proposed model can be extended to other countries to analyze and predict the trends of COVID-19 cases.

Keywords: COVID-19 pandemic, machine learning, deep neural network, reproduction number, particle swarm optimization

1.0 INTRODUCTION

Thailand, like many other countries, is currently grappling with the COVID-19 pandemic. To curb the spread of the virus, various measures have been implemented by authorities. Predicting the trajectory of the outbreak can assist decision-makers in formulating an effective response to the current and future waves of the infection. Several techniques have been developed by academics to model the spread of viruses, ranging from model-free methods [1, 2], mathematical models [3, 4], statistical models [4, 5, 6], to machine learning (ML) [5, 6, 7, 8, 9, 10, 11, 12].

However, the nonlinear trends in the evolution of COVID-19 are impacted by several factors, including cluster explosions, the effects of control measures, and virus mutants. Linear predictors and smooth average trends of mathematical and statistical models may limit the predictive performance. Therefore, the ML-based models, especially neural network (NN) models [9, 10, 11, 12, 13, 14], have been demonstrated to be more effective in characterizing COVID-19 cases. Shallow NNs, also known as feedforward NNs, have been widely used in a timely fashion. However, SNNs with a small number of hidden layers may not capture nonlinearities sufficiently, which can be improved by using deep feedforward NNs (DNNs) with multiple hidden layers. To date, DNNs have not been used for COVID-19 predictions.

In the literature, DNNs have been applied successfully to prediction problems. However, their performance may suffer from the vanishing gradient problem (VGP) and overfitting during training using the backpropagation algorithm (BPA). Additionally, longer periods of training are required to continue characterizing

the remaining trends, which may not be timely for advance planning. Moreover, the lack of COVID-19 outbreak data in the early phase of infection limits the training of DNNs. Most NN models do not consider time independence in the COVID-19 time series, which considerably affects model accuracy. Furthermore, their hyperparameters, which improve the learning ability, cannot be determined analytically, and are often tuned through trial and error, which may not yield optimal performance.

In this study, a prediction model based on a deep neural network (DNN) is applied to estimate the final epidemic size and evolving trends of confirmed COVID-19 cases for the first through fifth waves in Thailand. To make the model practical in the early phase, a one-day-ahead prediction is performed for short-term forecasting in the presence of a small amount of COVID-19 data. Based on the forecasted future epidemic trends, the previously predicted values are incorporated into the predictor set to estimate the next consecutive values, which are then repeated until convergence. The dynamics of the effective reproduction number, which assesses the severity of virus transmission, are estimated using mathematical demography with these predicted values. To train the DNN effectively, outbreak data from other countries that have passed the peak of infection under viral mutants are selected and included in the training dataset. Additionally, a particle swarm optimization (PSO) is employed to derive optimal hyperparameters, including input time-lag. Furthermore, a dropout regularization technique is used to address the vanishing gradient problem (VGP) while reducing model complexity. The prediction performances of the proposed dropout DNN-PSO are compared with those of conventional neural networks and the methods used in previous studies [2, 7].

2.0 METHODOLOGY

Active COVID-19 case data for Thailand were collected from the Department of Diseases Control, Ministry of Public Health, Thailand, while those for other countries were sourced from the Worldometer website. A rigorous process was followed to ensure that only relevant and reliable data were included in the dataset, based on the similarity among the data. To ensure that the dataset was standardized, maximum and minimum values outside the data range were identified and used to normalize the data, thereby removing the variability in the scales of the predictors. The normalization process ensures that the data used in the analysis are in a consistent format and facilitate better comparisons between different data points.

The prediction model for COVID-19 cases is shown in Figure 1 and can be expressed mathematically as follows:

$$\hat{S}_{t+1} = f(\hat{S}_t, \hat{S}_{t-1}, \ldots, \hat{S}_{t-N}) + \varepsilon_{t+h}\,, \tag{1}$$

where $\hat{S}_{t+1}$ represents the predicted value as a function of the historical values ($\hat{S}_t, \ldots, \hat{S}_{t-N}$), N is the maximum time lag, and ε denotes errors. Based on the estimated trend and final epidemic size, the predicted value is used as the predictor set to predict the next consecutive day and repeated until convergence. To prevent error propagation, a tracking list is used to store some of the predicted values while checking them against actual data. The prediction model based on DNN is detailed in the following subsections.

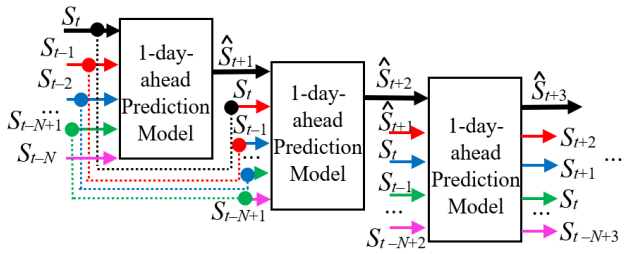

Figure 1 One-day-ahead predictions to formulate a new predictor set using the predicted values for predicting consecutive values

The shallow neural network (SNN) - comprising only a few hidden layers - has limitations as a prediction model and can only be used in countries that experienced the first peak of the COVID-19 outbreak [9, 10]. In contrast, the deep neural network (DNN) - with a larger number of hidden layers - is a viable alternative. However, deep learning models are susceptible to the vanishing gradient problem (VGP), where the gradient of the error function, denoted as $\nabla e(x)$, becomes close to zero through iterative multiplication. To address this issue, unsquashing functions, such as the rectified linear unit (ReLU(x) = max[0, x]) and exponential linear unit (ELU(x) = max[a(e^x-1), x]), where a is a positive constant, are incorporated into the activation function set ψ = {tanh, σ, ReLU, ELU}. These functions improve learning while preserving nonlinear transformation. Additionally, traditional squashing functions such as the hyperbolic tangent (tanh) and sigmoid (σ) functions are also included.

Additionally, when the DNN has a small set of training data, overfitting can occur, causing the model to memorize the training data and failing to predict unseen data. To improve deep learning and reduce DNN complexity, the dropout regularization technique is used [15]. This technique removes redundant hidden nodes in each layer with probability $p^{(l)}$, where l = 1, 2, ..., L (maximum hidden layer). The hidden nodes are randomly removed temporarily with the dropout ratio 1-p (represented by the blacked nodes in Figure 2). It should be noted that p is the dropout rate written in Python language in Keras, a deep learning library. The dropout DNN generates 2^{HN} thinned DNNs, where $HN = N(\prod H^{(l)})$ is the number of hidden nodes. The dropout DNN can be expressed as follows:

$$\hat{S}_{DNN}(t+1) = \sum_{k=1}^{H^{(L)}} w_{k1}^{(L)} \frac{\mathbf{D}^{(l)}}{1-p^{(l)}} \phi\,, \tag{2}$$

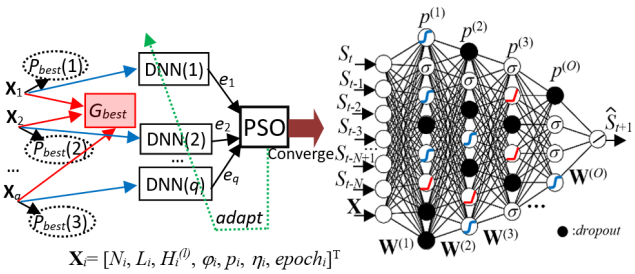

Figure 2 DNN-based prediction model with dropout technique optimized by PSO

where

$$\phi = \psi_k^{(o)} \sum_{j=1}^{H^{(L-1)}} w_{jk}^{(L)} \psi_j^{(L)} \cdots \psi_i^{(1)} \left(\sum_{l=0}^{N} w_{il}^{(1)} S(t-l) \right), \quad (3)$$

and $\mathbf{D}^{(l)} : D_n^{(l)} \sim Bernoulli(p^{(l)})$, n = 1,2, …, $H^{(l)}$.

In BPA, the DNN is trained under the criterion,

$$Min\, J = \sum_i \left\| S_{t+i} - \hat{S}_{t+i} \right\|, \quad (4)$$

where S_{t+i} is the actual cases.

The connected weights of the dropout DNN are updated at $iter^{th}$-iteration as,

$$\mathbf{W}_{iter}^{(l)} \leftarrow \mathbf{W}_{iter}^{(l)} + \eta \mathbf{D}^{(l)} \frac{\partial J}{\partial \mathbf{W}^{(l)}}, \quad (5)$$

where η is the learning rate.

Given that confirmed COVID-19 cases exhibit a smooth *S*-shaped trend, a DNN structure with moderate hidden layers that require only a moderate number of hidden nodes is adequate. The hyperparameters, including N, L, $H^{(l)}$, ψ, p, η, and *epoch*, are optimized to enhance the DNN's performance. The search space has 2L+18 dimensions, encompassing L hidden nodes in each hidden layer, four activation functions (ψ) in combinations, L dropout ratios for each hidden layer, and three hyperparameters, including time lag (N), learning rate (η), and epoch (*epoch*). Nonetheless, optimizing DNN, especially when it varies with L, requires a simple and effective approach. Therefore, we employ PSO, a bio-inspired swarm intelligence, due to its simplicity and fewer required parameters.

In the PSO procedure (depicted in Figure 3), N_p-particles are initialized, each possessing hyperparameters of a (2L+18)-element position vector ($\mathbf{X}q$), for the dropout DNN, where q = 1, …, N_p. At the i^{th}-iteration, the q^{th}-particle moves with velocity $\mathbf{V}_q$ from Location 1 to Location 2 (along the yellow line). The fitness function J (Equation 6) evaluates each particle's fitness, and the personal best vector ($\mathbf{P}_{best}(i)$) and the global best scalar (G_{best}) are updated accordingly. If $P_q(i) > P_{best,q}(i-1)$, $P_{best,q}(i) = P_q(i)$; and if $P_q(i) > G_{best}(i)$, $G_{best}(i) = P_{best,q}(i)$. This process is repeated for a maximum of itermax iterations (i = 1, …, $iter_{max}$).

$$V_q(i+1) = \omega V_q(i) + c_1 P_{best,q}(i) + c_2 G_{best}(i) - c_{12} X_q(i), \quad (7)$$

$$\mathbf{X}_q(i+1) = \mathbf{X}_q(i) + \mathbf{V}_q(i+1), \quad (8)$$

respectively, where ω is inertia weight, c_1 and c_2 are acceleration constants, and c_{12}=c_1–c_2. Typically, ω < 1, c_1 and $c_2 \in$ [1, 3] and they are predefined and fixed. The process terminated when met the stopping criteria.

The basic reproduction number (R_0) and effective reproduction number ($R(t)$) are key epidemiological parameters used to quantify the average number of new infections caused by an infected individual. These parameters are essential in assessing the severity of pandemics and evaluating the effectiveness of control measures. Estimation of $R(t)$ can be achieved through various methods, including the mathematical demography approach proposed in [16]. Here, we adopt the aforementioned method and utilize the predicted cumulative cases obtained from the DNN to evaluate $R(t)$.

$$R(t-t_0) = \frac{\hat{I}(t)}{\sum_{a=u}^{a=v} \hat{I}(t-t_0) W(a)}, \quad (9)$$

where

$$W(a) = g e^{-ga} / (e^{-gu} - e^{-gv}), \quad (10)$$

$\hat{I}(t) = \hat{S}(t) - \hat{S}(t-1)$ is the predicted new case on day t, t_0 is the days lag of reported cases after the infection date, g is the mean duration of illness (the reciprocal of the recovery rate), and [u, v] denotes the infection duration. To simulate $R(t)$, g = 0.1 taken from the WHO (2020), which may be changed in the future.

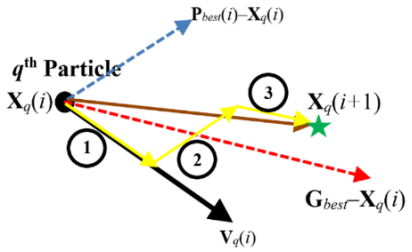

Figure 3 PSO-based selection optimal hyperparameters for DNN

Two metrics are commonly employed to evaluate the accuracy and goodness-of-fit of a model: the root mean square error (RMSE) (Equation 11) and the coefficient of determination (R^2) (Equation 12). A lower RMSE and a higher R^2 are indicative of a better prediction model. Thus, these metrics are essential for assessing the performance of a model.

$$RMSE = \sqrt{\frac{\sum_i (S_i - \hat{S}_i)^2}{N}}, \quad (11)$$

$$R^2 = 1 - \frac{\sum_i (S_i - \hat{S}_i)^2}{\sum_i (S_i - \bar{S}_i)^2}, \quad (12)$$

where $\bar{S}$ is the mean of the measured data.

In addition to assessing the accuracy of a model, evaluating the reliability of its predictions is also of utmost importance. Among the various reliability tests, test-retest reliability is the most widely utilized method. This test measures the consistency of predicted results over time, using the same dataset in model training. Test-retest reliability is commonly assessed through the calculation of the Pearson correlation coefficient.

$$r = \frac{\sum_i (\hat{S}_{1,i} - \bar{S}_{1,i}) - (\sum_i \hat{S}_{2,i} - \bar{S}_{2,i})}{\sqrt{\sum_i (\hat{S}_{1,i} - \bar{S}_{1,i})^2 \sum_i (\hat{S}_{2,i} - \bar{S}_{2,i})}}, \quad (13)$$

where $\hat{S}_{1,i}$, $\hat{S}_{2,i}$ are the predicted results of the test and retest, respectively, and $\bar{S}_{1,i}$, $\bar{S}_{2,i}$ are the mean values of them.

However, Equation (13) can be repeated, and the results averaged. Generally, *R*-values falling within the ranges of [0-0.4), [0.4-0.70), [0.7-0.9), and [0.9-1] indicate low, moderate, high, and very high correlations, respectively.

3.0 RESULTS AND DISCUSSION

The optimal hyperparameters set, θ = {*N*, *L*, $H^{(l)}$, ψ, *p*, η, λ, *epoch*}, selected among the combinations are shown in Table 1.

Table 1 Selecting hyperparameters of the DNN using PSO

θ	Range	Optimal values				
		Wave1	Wave2	Wave3	Wave4	Wave5
N	[2, 20]	8	10	8	6	5
L	[2, 10]	4	6	5	5	5
$H^{(l)}$	[10, 100]	10, 10, 13, 8	8, 12, 17, 20, 14, 19	14, 16, 25, 22, 17	10, 15, 27, 18, 23	12, 12, 14, 15, 7
ψ	{ReLU, ELU, tanh, σ}	{ReLu, tanh}	{ReLu, tanh}	{ELU, tanh, σ}	{ELU, tanh, σ}	{ReLu, tanh, σ}
p	[0.1, 0.5]	0.15, 0.30, 0.35, 0.27	0.13, 0.23, 0.29, 0.05, 0.13, 0.11	0.15, 0.32, 0.18, 0.13, 0.2	0.09, 0.18, 0.43, 0.11, 0.15	0.09, 0.15, 0.27, 0.15, 0.29
η	[10^{-3},0.1]	0.0015	0.0018	0.0028	0.0017	0.0031
epoch	[500,10^4]	5,000	10,000	7,500	6,500	5,500

At the initial stages of the first wave of infection, there was insufficient training data available for the NNs. As a result, training data were obtained from countries such as China, India, Hong Kong, and South Korea. To ensure preliminary similarity checks, cross-correlation indices were computed using outbreak data from China, Hong Kong, Korea, and India, with offsets ranging from 0 to 48-time lags, respectively. The results revealed that outbreak data from China and Korea demonstrated high similarities to Thailand, with cross-correlation indices of approximately 0.8717 (0-lag) and 0.7487 (24-lag), respectively.

The DNN-PSO model was trained using outbreak data from China and Korea (Figure 4). Figure 5 illustrates a comparison of prediction results between the proposed DNN-PSO model, DNN, SNN, and previous studies, including the logistic model [2] and the logistic regression model optimized by genetic algorithm (LGR/GA) [7]. Performance indices for each model are presented in Table 2. The proposed DNN-PSO model outperformed the other models in terms of low estimated error of the epidemic size (RMSE) and a high-fit model with a higher R^2-value.

The estimated *R*(*t*) values obtained from the DNN-PSO, DNN, and SNN models exhibit a gradual decline over time and are similar to the measured values, as depicted in Figure 6.

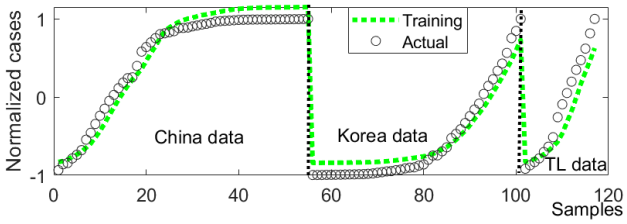

Figure 4 The training results of the DNN-PSO model using outbreak data as predictors from China and Korea for Thailand's first wave of COVID-19

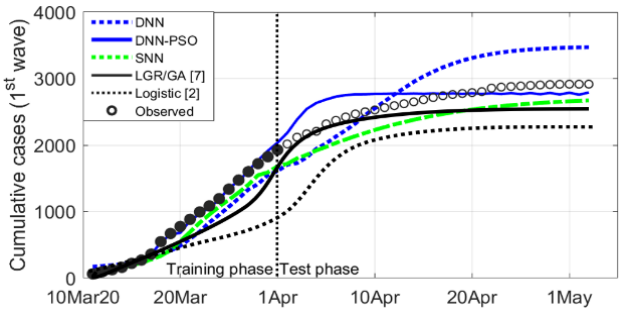

Figure 5 Prediction results of the DNN-PSO, DNN, SNN, and previous studies [2, 7] for Thailand's first wave of cumulative COVID-19 cases

Table 2 Performance of the prediction models for Thailand's first wave of COVID-19.

Model	Final epidemic size		Developed trends	
	Forecast	Error*	RMSE	R^2
DNN-PSO	2857	60	233.7	0.933
DNN	3500	583	345.3	0.892
SNN	2607	310	265.5	0.927
LGR/GA [7]	2532	385	332.7	0.873
Logistic [2]	2298	619	457.3	0.732

*Actual final epidemic size = 2,917

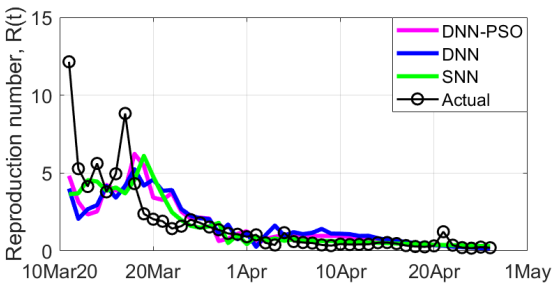

Figure 6 Reproduction numbers obtained from DNN-PSO, DNN, and SNN with the actual data for Thailand's first wave of COVID-19

The second wave of infections began with initial fluctuations in the number of daily infected cases, as shown in Figure 7, causing multiple peaks, and deforming the *S*-shaped curve of cumulative cases. To address this issue, outbreak data from countries that experienced the second wave before Thailand, including China, Hong Kong, Korea, and India, were included in the predictor set. Cross-correlation indices with offset time lags between the outbreak data of those countries and Thailand's first and second

waves were calculated, with values ranging from 0.778 to 0.93. During the training phase, the outbreak data from India was found to be the best predictor. During the testing phase, the proposed DNN-PSO outperformed other models, except for DNN, which had oscillations that accidentally touched the desired value. The proposed model exhibited a low estimated error and RMSE, as well as a high R^2 for estimating the final size and characterizing the developed trends, as shown in Figure 8 and Table 3. The other models underestimated the final epidemic size because their predictions were trapped in the first peak.

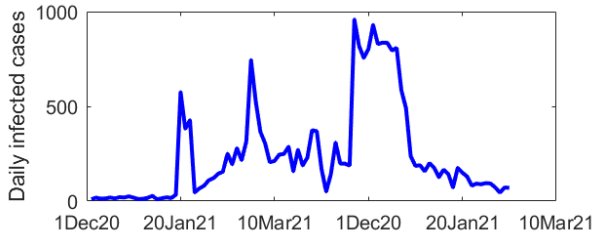

Figure 7 Multiple peaks of daily new infected cases of Thailand's second wave of COVID-19

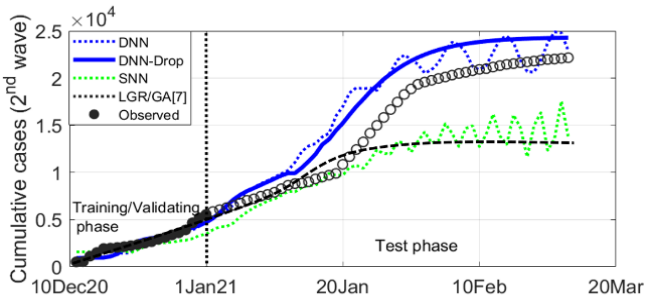

Figure 8 Prediction results of the DNN-PSO, DNN, SNN, and previous study [7] for Thailand's first wave of cumulative COVID-19 cases

Table 3 The comparison of performance between the prediction models for Thailand's second wave of COVID-19

Model	Final epidemic size		Developed trends	
	Forecast	Error*	RMSE	R^2
DNN-PSO	2.428×10^4	2,119	2,422	0.984
DNN	2.289×10^4	730	2,620	0.948
SNN	1.378×10^4	8,382	4,248	0.940
LGR/GA [7]	1.368×10^4	8,372	3,473	0.934

*Actual final epidemic size = 22,162

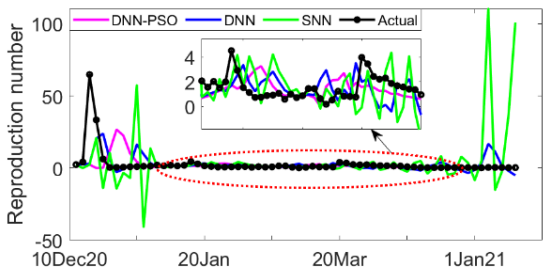

Figure 9 Reproduction numbers obtained from DNN-PSO, DNN, and SNN with the actual data for Thailand's second wave of COVID-19

Additionally, the DNN and SNN exhibited a more oscillating trend. However, the estimated $R(t)$ values obtained from all prediction models differed from the actual data due to prediction errors, as shown in Figure 9.

Following the third wave, the Delta variant became the dominant strain in Thailand, causing a rapid increase in the number of cases. Outbreak data from countries with high Delta variant cases, such as India, the UK, and the USA, were included in the training dataset, along with Thailand's previous waves. The cross-correlation indices between the outbreak data from India, the UK, the USA, and Thailand's previous waves with the beginning of the fourth wave in Thailand are about 0.944 (0-lag), 0.908 (0-lag), 0.834 (32-lag), and 0.974 (0-lag), respectively.

In the testing phase, the DNN-PSO model outperformed the other models in terms of a low estimated error and RMSE, as well as a high R^2 for estimating the final size and characterizing the developing trends (Figure 12 and Table 5). The estimated $R(t)$ values obtained from all models are in good agreement with the actual data (Figure 13). However, the predictions for the peak and the end of the fourth wave may be revised due to the unpredictable nature of the pandemic.

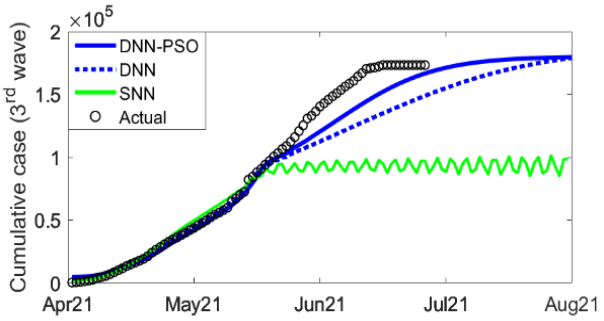

Figure 10 Prediction results of the DNN-PSO, DNN, and SNN for Thailand's third wave of cumulative COVID-19 cases

Table 4. Performance of the prediction models for Thailand's third wave of COVID-19.

Model	Final epidemic size		Developed trends	
	Forecast	Error*	RMSE	R^2
DNN-PSO	1.667×10^5	6.49×10^3	1.16×10^3	0.993
DNN	1.489×10^5	2.44×10^4	1.95×10^4	0.983
SNN	1.08×10^4	1.62×10^5	8.75×10^5	0.735

*Actual final epidemic size = 173,349

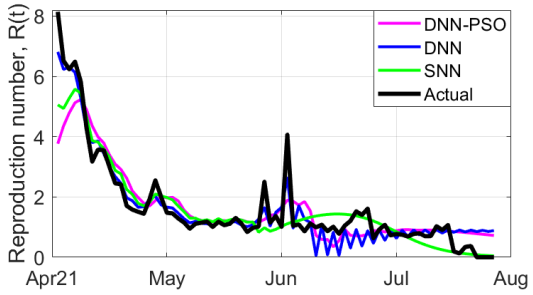

Figure 11 Reproduction numbers obtained from DNN-PSO, DNN, and SNN with the actual data for Thailand's third wave of COVID-19.

During Thailand's fourth wave of infection, which was caused by the Delta variant, there was a rapid increase in COVID-19 cases. Although the previous three waves provided sufficient training data, the prediction models did not perform as expected in the prediction phase. To address this, outbreak data from countries with highly similar patterns to Thailand's fourth wave, such as India, the UK, South Africa (SA), the USA, Australia (Aus.), and others, were included in the training dataset along with data from Thailand's previous three waves. The cross-correlation between the outbreak data from these countries and Thailand's fourth wave was approximately 0.919 (230-lag) for India, 0.904 (33-lag) for SA, 0.889 (69-lag) for Aus., and 0.865 (149-lag) for the UK. During the training phase, the outbreak data from all these countries provided the best predictor set.

In the test phase, the DNN-PSO model outperformed the others in terms of low RMSE and error variance, characterizing the developing trends (Figure 12 and Table 5). However, high errors were observed in the overestimation of epidemic trends during the middle wave of this wave for the DNN-PSO. This is due to the provision of sufficient vaccines to individuals, thereby reducing the number of susceptible individuals. The estimated R(t) values obtained from the DNN-PSO models were close to the actual data in the initial phase but quite different in the rest of the phase (Figure 13). The estimated $R(t)$ corresponding to the convergence to the final size too early indicates that the outbreak terminated too early, which needs further improvement. Additionally, the estimated $R(t)$ values of the DNN, for which the estimated trends are like those of the measures, were fairly close to the actual values.

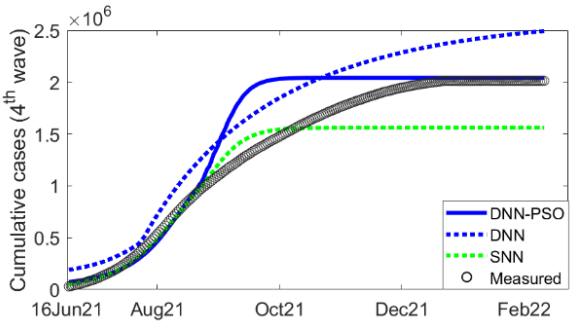

Figure 12 Prediction results of the DNN-PSO, DNN, and SNN for Thailand's fourth wave of cumulative COVID-19 cases

Table 5 Performance of the prediction models for Thailand's fourth wave of COVID-19

Model	Final epidemic size		Developed trends	
	Forecast	Error*	RMSE	R^2
DNN-PSO	2.043×10^6	3.03×10^4	1.95×10^5	0.926
DNN	2.493×10^6	4.80×10^5	3.31×10^5	0.997
SNN	1.562×10^6	4.51×10^5	2.74×10^5	0.921

*Actual final epidemic size = 2,012,738

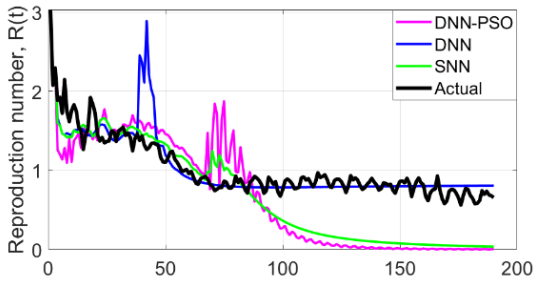

Figure 13 Reproduction numbers obtained from DNN-PSO, DNN, and SNN with the actual data for Thailand's fourth wave of COVID-19

In the current wave of the epidemic, concerns are mounting due to the emergence of the Omicron variant. To forecast the cumulative number of infected cases, the training dataset incorporates data from the previous four waves of outbreaks. However, the resulting prediction outcomes exhibit large errors, primarily because of the evolution of disease transmission arising from the distinct infection characteristics of each wave. Consequently, outbreak data from countries severely affected by the Omicron variant, including South Africa, Nigeria, and the USA, are included in the training dataset.

During testing, the DNN-PSO model outperforms other models, exhibiting a low estimated error and root mean square error (RMSE), as well as a high coefficient of determination (R^2) for estimating the final size and characterizing the developing trends (Figure 14 and Table 6). The estimated $R(t)$ values obtained from all models closely align with the actual data (Figure 15).

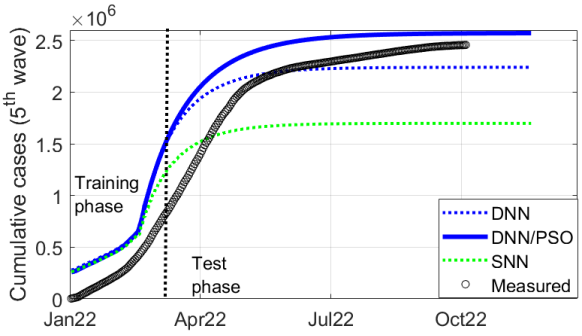

Figure 14 Prediction results of the cumulative cases for the fifth wave of infection from the proposed models.

Table 6 Performance of the prediction models for Thailand's fifth wave of COVID-19.

Model	Final epidemic size		Developed trends	
	Forecast	Error*	RMSE	R^2
DNN-PSO	2.55×10^6	9.06×10^4	3.54×10^5	0.96
DNN	2.20×10^6	2.53×10^5	4.94×10^6	0.93
SNN	1.64×10^6	8.12×10^5	5.08×10^5	0.91

*Actual final epidemic size = 2,456,727

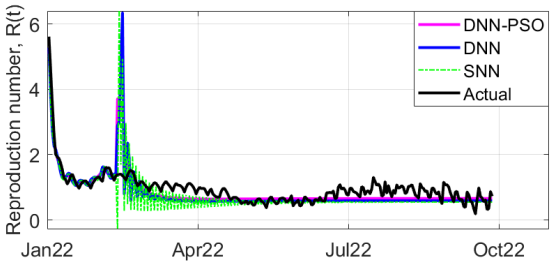

Figure 15 Reproduction numbers obtained from DNN-PSO, DNN, and SNN with the actual data for Thailand's fifth wave of COVID-19

To ensure the accuracy of the one-day forecast values before incorporating them into the training dataset for predicting the cumulative cases in the five-wave COVID-19 epidemic, a comprehensive evaluation process is employed. This process involves comparing the forecasted values with actual data to identify any discrepancies within an acceptable range. The dynamic nature of the epidemic's spread exhibits a distinctive pattern, characterized by an initial increase followed by a subsequent decrease, with varying durations for each wave, except in cases with intervening measures. Error propagation is critical and is addressed by implementing a tracking list cross-referenced with actual data to evaluate prediction performance effectively. The intricate interplay of various factors influencing the epidemic's spread poses challenges in determining the number of 1-day forecasts utilized in each outbreak wave. The iterative and meticulous forecasting process persists until the final number of infected individuals approaches zero (R<1) or reaches an equilibrium constant (R>1), signifying a transition into an endemic state, warranting continuous monitoring and adaptation of the forecasting model.

4.0 CONCLUSION

This paper proposes a dropout DNN-PSO model to estimate the final epidemic size and characterize the developing trends of cumulative COVID-19 cases in Thailand's first to fifth waves of infection. The proposed model outperforms other models; however, it needs to be improved to capture the dynamics of the epidemic beyond nonlinear transformation. As COVID-19 exhibits nonlinear trends that vary over time due to several factors, it is a time-series in which future values depend on past occurrences. To enhance the model's performance, exogenous data that affect the outbreak, such as the number of administered vaccines, can be integrated into the predictor set. Furthermore, implementing other ML models with memory units in the structure, such as the recurrent neural network (RNN), can lead to more efficient predictive models.

Acknowledgement

This research is fully supported by The Research Institute of North-Chiang Mai University.

References

[1] Roosa, K., Lee, Y., Luo, R., Kirpich, A., Rothenberg, R., Hyman, J. M., Yang, P., and Chowell, G. 2020. Short-term forecasts of the COVID-19 epidemic in Guangdong and Zhejiang, China: February. *Journal of Clinical Medicine*. 9(596):13-23. DOI: 10.3390/jcm9020596

[2] Wongsathan, R. 2021. Real-Time prediction of the COVID-19 epidemic in Thailand using simple model-free method and time series regression model. *Walailak Journal of Science and Technology*. 18(14): 1-11 DOI: 10.48048/wjst.2021.10028

[3] Rahimi, I., Gandomi, A. H., Asteris, P. G., and Chen, F. 2021. Analysis and prediction of COVID-19 using SIR, SEIQR, and machine learning models: Australia, Italy, and UK cases. *Information*. 12: 1-23. DOI: 10.3390/info12010001

[4] Abolmaali, S., and Shizaei, S. 2021. A comparative study of SIR model, linear regression, logistic function and ARIMA model for forecasting COVID-19 cases. *AIMS Public Health Journal*. 8(4): 598-613. DOI: 10.3934/publichealth.2021049

[5] Khoojine, A. S., Shadabfar, M., Hosseini, V. R., and Kordestami, H. 2021. Autoregressive model for the prediction of COVID-19 considering the disease interaction in neighboring countries. *Entropy*. 23: 1-18. DOI: 10.3390/e23010048

[6] Swapnarekha, H., Beher, H. S., Nayak, J., Naik, B., and Kumar, P. S. 2021. Multiplicative Holts Winter model for trend analysis and forecasting of COVID-19 spread in India. *Springer Nature Computer Science Journal*. 2(416): 1-15. DOI: 10.1007/s42979-021-00614-7

[7] Wongsathan, R. 2023. The logistic growth regression model with the genetic algorithm for predicting the third wave of the COVID-19 epidemic in Thailand. *Asia-Pacific Journal of Science and Technology*. 28(1): 1-16. DOI: 10.14456/apst.2023.1

[8] Kafieh, R., Arian, R., Saeedizadh, N., Amini, Z., Serej, N. D., and Minaee, S. 2021. COVID-19 in Iran: forecasting pandemic using deep learning. *Computational and Mathematical Methods in Medicine*. 1-16. DOI: 10.1155/2021/6639466

[9] Wieczorek, M., Siłka, J., Połap, D., Woźniak, M., and Damas˘evičius, R. 2020. Real-time neural network based predictor for cov19 virus spread. *Public Library of Science ONE*. 15(12): e0244116. DOI: 10.1371/journal.pone.0244116.

[10] Niazkar, H. R., and Niazkar, M. 2020. Application of artificial neural networks to predict the COVID-19 outbreak. *Global Health Research and Policy*. 5: 1-11. DOI: 10.1186/s41256-020-00177-4

[11] Alamsyah, A., Prasetiyo, B., Hakim, M. F. A., and Pradana, F. F. 2021. Prediction of COVID-19 using recurrent neural network model. *Scientific Journal of Informatics*. 8(1): 1-6. DOI: 10.15294/sji.v8i1.30599

[12] Priyanka, A., and Kumari, M. S. 2021. Implementation of simple RNN and LSTMs based prediction model for coronavirus disease (COVID-19). *IOP Conf Series: Materials Science and Engineering*. 1022: 012019. DOI: 10.1088/1757-899X/1022/1/012032

[13] Kumar, R. L., Khan, F., Din S., Band, S. S., Mosavi, A., and Ibeke, E. 2021. Recurrent neural network and reinforcement learning model for COVID-19 prediction. *Frontier in Public Health*. 9: 1-12. DOI: 10.3389/fpubh.2021.615392

[14] Li, Q., and Lin, R. C. 2016. A new approach for chaotic time series prediction using recurrent neural network. *Mathematical Problem in Engineering*. 1-9. DOI: 10.1155/2016/8459014

[15] Srivastava, N., Hinton, G., Krizhevsky, A., and Sutskever, I., Salakhutdinov R. 2014. Dropout: A simple way to prevent neural networks from overfitting. *Journal of Machine Learning Research*. 15: 1929-58. DOI: 10.5555/2627435.2670313

[16] Rosero-Bixby, L., and Miller, T. 2022. The mathematics of the reproduction number R for COVID-19: *A primer for demographers. Vienna Yearbook of Population Research*. 20: 143-166. DOI: 10.1553/populationyearbook2022s143